Preparation of Spherical Oxalate Particles of Rare Earths in Emulsion Liquid Membrane System

Takayuki Hirai, Norihiko Okamoto, and Isao Komasawa
Dept. of Chemical Science and Engineering, Osaka University, Osaka 560, Japan

Submicron-sized spherical oxalate particles of rare earths were prepared by using an emulsion liquid membrane (ELM, (water-in-oil-in-water (W/O/W) emulsion) system, consisting of Span 83 (sorbitan sesquioleate) as a surfactant and EHPNA (2-ethylhexylphosphonic acid mono-2-ethylhexyl ester) as an extractant (cation carrier). Rare-earth ions were extracted from the external water phase and stripped into the internal water phase to make submicron-sized oxalate particles. In the case of Ce, Pr, Nd, Sm, and Gd, well-defined spherical oxalate particles (0.2–0.6 μm dia.) were obtained, following the formation of primary particles of about 20 nm. In contrast, less spherical or rather tabular particles were formed for La, Dy, and Y, possibly owing to their formation in the external phase following some breaking of the water-in-oil (W/O) emulsion drop. Oxalate particles of Yb were not obtained in this system. Effects of the internal water droplet size, the rare-earth ion concentration in the external water phase, and the volume ratio of organic membrane phase to internal water phase of the W/O emulsion (O/A ratio), on the size of spherical particles, were investigated. A simulation study based on the model of transport mechanism of rare-earth ions through the organic membrane phase revealed that the particle size was determined by the distribution of rare-earth ions into the internal water droplets, as confirmed by the experimental results. The control of the particle size was found to be feasible by control of the feed rare-earth concentration and size of the internal water droplets.

Introduction

An emulsion liquid membrane (ELM, water-in-oil-in-water (W/O/W) emulsion) system has been studied for the selective separation and concentration of metals, where the metal ions in the external water phase are extracted into the organic membrane phase and then stripped into the internal water phase. Recently, it has been found that the internal water phase is capable of being used to prepare size-controlled and morphology-controlled fine particles such as precious-metal particles (Majima et al., 1991), copper oxalate particles (Yang et al., 1991; Stewart and Davies, 1992; Hirai et al., 1996), and calcium carbonate particles (Davey and Hirai, 1997; Hirai et al., 1997). In previous work (Hirai et al., 1996), submicron-sized (0.18–0.50 μm in diameter) copper oxalate particles were obtained, which were aggregates of primary particles of about 8 nm. The size of the particles could be controlled by varying the O/A ratio of the water-in-oil (W/O) emulsion, which is defined as the volume ratio of organic membrane phase to internal water phase.

Oxalate particles of rare-earth elements are also important materials in such industrial applications as the precursors of rare-earth oxides, since oxalates give oxides readily by calcination. Recently, the precipitation stripping of lighter rare-earth elements such as La to make oxalate particles has been reported, as well as that of heavier rare earths such as Y (Yoon and Doyle, 1988, 1990, 1992; Lee and Doyle, 1991; Doyle et al., 1993). For La, $La_2(C_2O_4)_3$ particles were obtained from an organic kerosene solution containing La-loaded neodecanoic acid by contact with an aqueous solution containing dimethyloxalate or oxalic acid. Span 20 (sorbitan monolaurate), Span 60 (sorbitan monostearate), or Tween 80 (polyoxyethylene-20-sorbitan monooleate) were used as surfactant to form a W/O or O/W emulsion. This was done by mechanical stirring and ultrasonic agitation, when contacting the organic phase with aqueous phase and aiming to control

Correspondence concerning this article should be addressed to T. Hirai.

the particle size. However, the control of size and morphology of the particles was found to be fairly difficult, probably because some precipitation occurred before a stable emulsion was formed by the agitation. Thus the particles formed had a characteristic lath shape and developed to several microns in size. For Nd, Konishi et al. (1993a,b) reported that $Nd_2(C_2O_4)_3$ particles were obtained by vigorous shaking of the organic solution, containing Nd-ioaded VA10 (tertiary monocarboxylic acid, Versatic 10) or EHPNA (2-ethylhexylphosphonic acid mono-2-ethylhexyl ester), with the oxalic acid solution. Particles of 1–5 μm in size, having a tabular and elongated shape were obtained, and were completely free from contamination by the extractant and organic solvent. The preparation of samarium oxalate particles from kerosene solutions of Sm-loaded D2EHPA (bis(2-ethylhexyl)phosphoric acid) or VA10 has also been reported (Sanuki et al., 1994). Needlelike precipitates of about 1–10 μm in size were obtained. It was also found that the particle size decreased with increasing oxalic acid concentration, probably owing to an increase in stripping rate. In general, this precipitation stripping method produces smaller-sized particles as compared to particles obtained from homogeneous aqueous systems. When employing an ELM system, which has micron-sized water droplets, it is expected that more size- and morphology-controlled fine particles should be obtained since the reaction area is restricted.

The preparation of oxalate fine particles of the rare earths, from La to Yb, using the ELM system was therefore investigated in this study. EHPNA, widely used in industrial rare-earth separation processes, was used as extractant. The various factors controlling the size and morphology of the particles were investigated. A simulation study, based on the model for the transfer mechanism of rare-earth ions through ELM, was also carried out, in order to clarify the main controlling factor in determining particle size.

Experimental Studies

EHPNA (supplied by Daihachi Kagaku Kogyo Co. Ltd., Osaka, with the commercial name of PC-88A) was used as the extractant, and sorbitan sesquioleate (Span 83, supplied by Tokyo Kasei Kogyo Co., Ltd., Tokyo) was used as the surfactant. Rare-earth nitrates ($Ln(NO_3)_3$) and oxalic acid were supplied by Wako Pure Chemical Industries, Ltd. The internal water phase for the emulsion (0.1 mol/L oxalic acid) and the organic membrane phase (kerosene containing 0.5 mol/L EHPNA and 5 wt. % Span 83) were mixed at a volume ratio of 1:1 or 2:1 (O/A ratio = 1 or 0.5) and were emulsified mechanically by use of a homogenizer (12,000 rpm). The resulting W/O emulsion (10 mL) was added to an external water phase (50 mL of $Ln(NO_3)_3$ aqueous solution, $[Ln]_0 = 100-1{,}000$ ppm) and was stirred vigorously by a magnetic stirrer to form a W/O/W emulsion. The size of the emulsion drops (< 2 mm), dispersed in the external water phase, was measured by photography during the course of stirring. The W/O emulsion was then separated from the external solution and demulsified by adding 20 mL of acetone. The particles, formed in the water droplets, were separated by centrifuge and were washed with acetone more than 3 times. The size of the internal water droplets and the particles obtained were measured by a laser-scattering particle-size distribution analyzer (Horiba LA-910W). The particles were also characterized with a scanning electron microscope (SEM, Hitachi S-5000), an X-ray diffractometer (Philips PW-3050), and a thermogravimeter/differential thermal analyzer (TG-DTA, Shimadzu TG-DTA 50). To determine the Ln concentration in each phase, the separated W/O emulsion was demulsified electrically and the organic membrane phase was then stripped with 0.1 mol/L HNO_3. The Ln concentration of the resulting aqueous solution and of the external aqueous solution was determined with an inductively coupled argon plasma atomic emission spectrometer (ICP-AES, Nippon Jarrell-Ash ICAP-575 Mark II). The Ln concentration in the internal phase was then estimated by mass balance.

Results and Discussion

Size and morphology of particles

Following the extraction of the Ln ions from the external water phase into the internal water phase, the following internal water phase reaction occurs and rare-earth oxalate particles are precipitated:

$$2Ln^{3+} + 3H_2C_2O_4 + nH_2O \rightarrow Ln_2(C_2O_4)_3 \cdot nH_2O + 6H^+. \quad (1)$$

SEM images of typical oxalate particles for Ce, Pr, and Nd, when obtained at an O/A ratio = 1 and a feed concentration of Ln ions in the external phase ($[Ln]_0$) = 500 ppm, are shown in Figure 1. Well-defined spherical particles mainly of 0.2–0.6-μm size were obtained. Similar particles were obtained for Sm and Gd. The particles obtained in homogeneous aqueous solution under similar concentration conditions, however, were not spherical but tabular and elongated, and of a size greater than 1 μm, as shown in Figure 2, for Pr oxalate. The ELM system is therefore effective in controlling both the particle size and the morphology. In contrast, spherical oxalate particles were not formed, even in the ELM system, for the heavier rare earths. Since the extractability of the heavier elements by EHPNA is greater than that of the lighter elements, the heavier elements such as Dy, Y, and Yb were not stripped effectively from the organic membrane phase with oxalic acid, and thus the longer stirring time was needed to make oxalate particles. Instead, tabular particles were obtained for Dy and Y, and their morphology appeared to be similar to that for particles formed in the homogeneous solution. This suggests that these particles may be formed in the external water phase, following possible breakage of the emulsion drop during the long stirring time. The heavier element, Yb, was not precipitated in the ELM system, since Yb is rarely stripped with oxalic acid any more. As for the lightest element, La, less spherical particles were obtained, which were the aggregates of smaller elongated particles. The present ELM system is therefore applicable to the preparation of oxalate spherical particles of rare earths from Ce to Gd.

XRD analysis of the oxalate particles for Ce, Pr, and Nd formed in the ELM system showed characteristic diffraction peaks of $Ce_2(C_2O_4)_3 \cdot 10H_2O$, $Pr_2(C_2O_4)_3 \cdot 10H_2O$, and $Nd_2(C_2O_4)_3 \cdot 10H_2O$, respectively. The particles showed TG-DTA profiles similar to those of the particles obtained in the homogeneous system. The spherical oxalate particles ob-

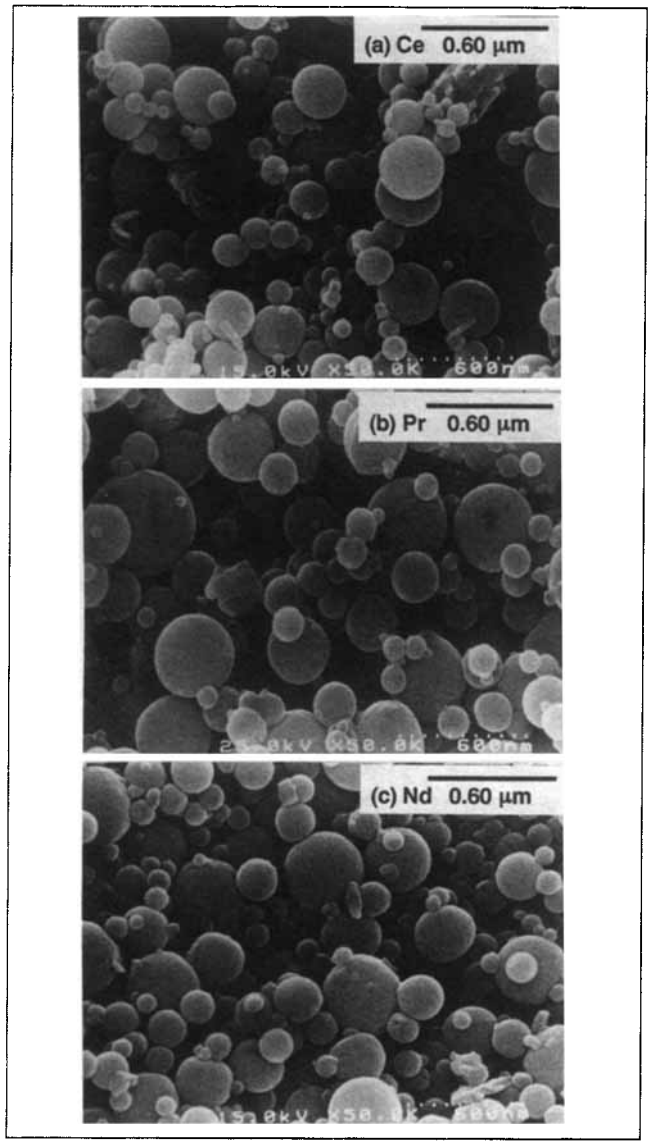

Figure 1. Scanning electron micrographs of oxalate particles for (a) Ce, (b) Pr, and (c) Nd prepared in the ELM system, with an O/A ratio = 1, $[Ln]_0$ = 500 ppm, and t = 2 h.

tained by the ELM system were calcined and then characterized by XRD and SEM, with the results shown in Figures 3 and 4, respectively. XRD patterns for the corresponding rare-earth oxides, CeO_2, Pr_6O_{11}, and Nd_2O_3, were observed. SEM observation revealed that calcination of the spherical Pr oxalate particles caused cavities by CO_2 elimination at 773 K, followed by particle fracture into smaller oxide particles and some sinter at 1,073 K.

Mechanism of particle formation

Figure 5 shows the time–course variation in the concentrations for Pr ions in the external water phase, organic membrane phase, and internal water phase, where $[Pr]_0$ = 500 ppm (about 3.5 mmol/L). The transport of Pr ions into the internal phase was completed in 10 min at O/A ratios of both 1

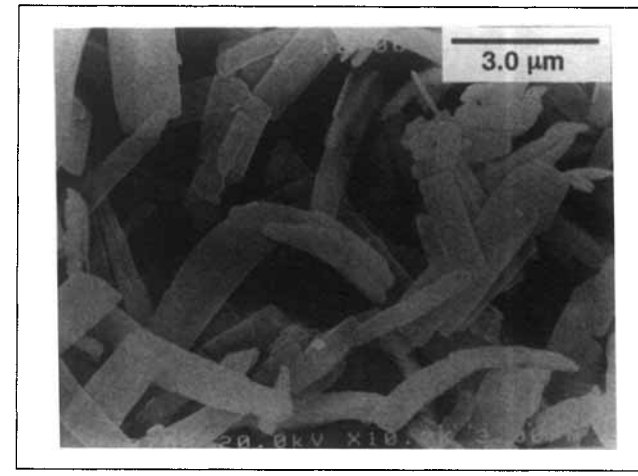

Figure 2. Scanning electron micrograph for Pr oxalate ($Pr_2(C_2O_4)_3 \cdot 10H_2O$) particles prepared in homogeneous aqueous solution by mixing of 50 mL of 500 ppm $Pr(NO_3)_3$ solution and 5 mL of 0.1 mol/L $H_2C_2O_4$ solution for 2 h.

and 0.5. Figure 6 shows the SEM images for the Pr oxalate particles, obtained at different reaction (stirring) times. At t = 15 min, mainly smaller particles of about 20 nm in size were observed, and were thought to be formed in the internal phase immediately after the transport of Pr ions. These primary particles then decreased in number, with increasing reaction time and almost disappeared following 2 h of stirring, as shown in Figure 1b. This result shows that the primary particles slowly aggregated together to form final spherical particles of 0.2–0.6 μm in size. The shape of the internal water droplets is likely to influence the morphology of the formed particles. The size of the spherical particles is, however, smaller than the size of the water droplets (about 1.84 μm at O/A ratio = 1 and 2.14 μm at O/A ratio = 0.5).

Effect of O/A ratio

The transport rate of Pr ions is slightly increased by increasing the O/A ratio, as shown in Figure 5. Although this tendency is similar to that of Cu ions (Hirai et al., 1996), the difference in the transport rate in the present case is slight. The drop diameter for the W/O emulsion decreases linearly with stirring time, possibly by the splitting of the drops into small drops, and is less at an O/A ratio = 1 (about 1 mm at t = 1 min and 0.7 mm at 10 min) than at 0.5 (about 1.9 mm at t = 1 min and 1.2 mm at 10 min). With increasing O/A ratio, that is, with increasing volume of the organic phase, a better W/O emulsion dispersion is obtained since the viscosity of the emulsion is decreased. Thus, for the extraction of Pr, the interfacial area increases at an O/A ratio = 1 and, thus, the transport rate is increased.

Figure 7 shows the SEM image for Pr oxalate particles when obtained at an O/A ratio = 0.5. Spherical particles were observed that were similar to the particles obtained at an O/A ratio = 1 and shown in Figure 1b, except that smaller primary particles were still observed, even at t = 2 h. The mean size of the particles is hardly influenced by the O/A ratio, as shown in Figure 8. This finding differs from the case of Cu oxalate

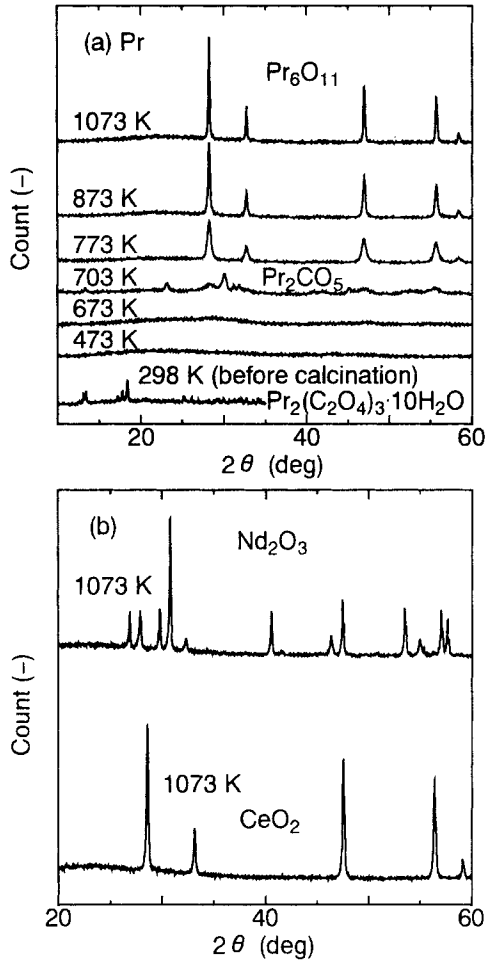

Figure 3. X-ray diffraction patterns of the particles before and after calcination of (a) Pr oxalate, and (b) Nd oxalate and Ce oxalate for 2 h at the shown temperature.

Particles were prepared in the ELM system with an O/A ratio = 1, $[Ln]_0$ = 500 ppm, and t = 2 h.

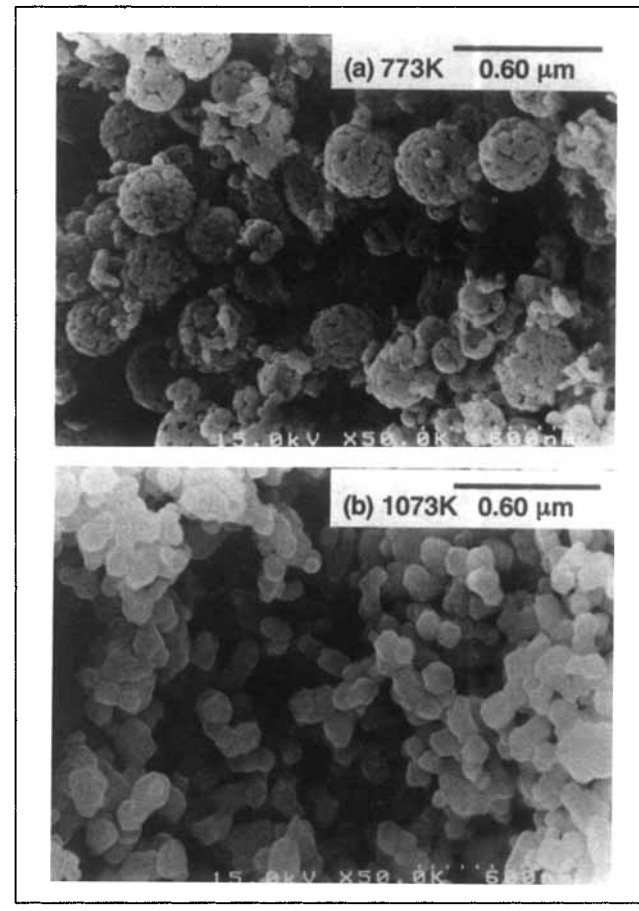

Figure 4. Scanning electron micrographs for Pr oxide particles obtained by calcination of Pr oxalate particles for 2 h at (a) 773 K and (b) 1,073 K.

Particles were prepared in the ELM system with an O/A ratio = 1, $[Ln]_0$ = 500 ppm, and t = 2 h.

(Hirai et al., 1996), in which the particle size is decreased markedly with increasing O/A ratio. In that case, the particle size was controlled by the distribution of Cu ions into the water droplets. This is because the submicron-sized secondary particles were formed by the processes of distribution, precipitation of smaller primary particles, and aggregation in the single water droplet, without interaction between two or more droplets. Assuming that a similar mechanism of particle formation applies in the present case, the distribution of Pr ions in the internal water droplets is unlikely to be influenced by the O/A ratio. To clarify this, the transport of rare-earth ions was investigated by model development and simulation.

Model development for the simulation of transport and precipitation of rare-earth ions in ELM system

The model of the particle formation process utilizes the extraction model for Cu ions in the ELM system proposed by Teramoto et al. (1983), with the addition of precipitation in the internal water phase. A similar model was applied to the formation process for Cu oxalate particles (Hirai et al., 1996). In this model, the W/O emulsion drops and internal water droplets are spherical and the water droplets are located uniformly in the emulsion drop and are immobile. The linear decrease in the emulsion drop size are taken into consideration. The elementary steps are as follows.

1. Diffusion of Ln^{3+} and H^+ through the stagnant film of the external water phase.
2. Formation of a complex between Ln^{3+} and the extractant at the interface between the external/membrane phases.
3. Diffusion of the complex and extractant in the peripheral oil layer of the emulsion drop.
4. Diffusion of the complex and extractant through the organic membrane phase.
5. Stripping of Ln^{3+} and the precipitation of rare-earth oxalate, by reaction between Ln^{3+} and oxalate ion. Dissociation of oxalic acid in the water droplets also occurs during the process of precipitation.

Breakage of the membrane is not taken into account in the model. The effective diffusivities for the extractant and the extracted species in the membrane phase are assumed to be constant. The mass-transfer resistance in the internal water

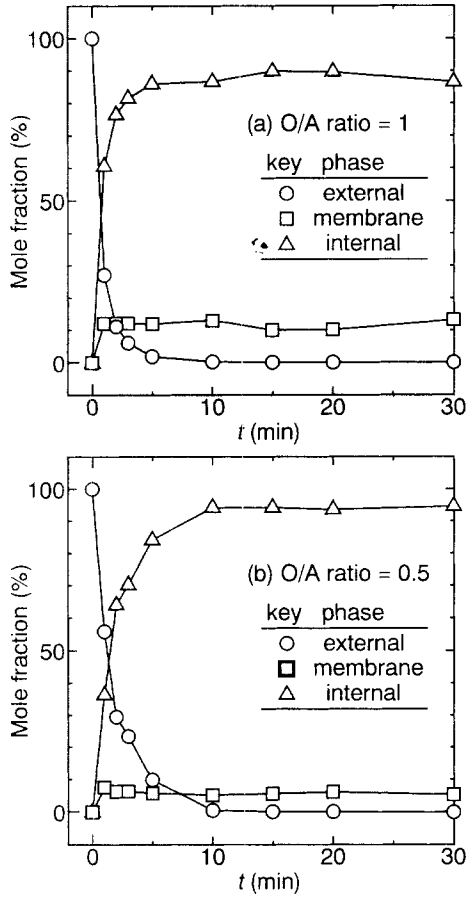

Figure 5. Time-course variation for the mole fractions of Pr ion in the external water phase, organic membrane phase, and internal water phase in the ELM system for the cases of $[Pr]_0 = 500$ ppm and O/A ratio = (a) 1 and (b) 0.5.

The mole fraction in the initial external water phase is set at 100%.

phase is neglected, because this phase is much smaller than the W/O emulsion drop.

The overall extraction equilibrium is formulated as shown in Eq. 2 where RH denotes EHPNA. With the concentrations of Ln^{3+}, dimer of free extractant, extracted species, and H^+ shown by A, B, C, and H, respectively, the extraction equilibrium constant and the rates of forward and reverse reactions are expressed by Eqs. 3–5, respectively:

$$Ln^{3+} + 3(\overline{RH})_2 \leftrightarrow \overline{LnR_3(RH)_3} + 3H^+ \tag{2}$$

$$K_{ex} = CH^3/AB^3 \tag{3}$$

$$r_f = k_f AB^3/H^3 \tag{4}$$

$$r_r = k_r C. \tag{5}$$

The balance equation for the Ln^{3+} in the external water phase (phase I) is given by

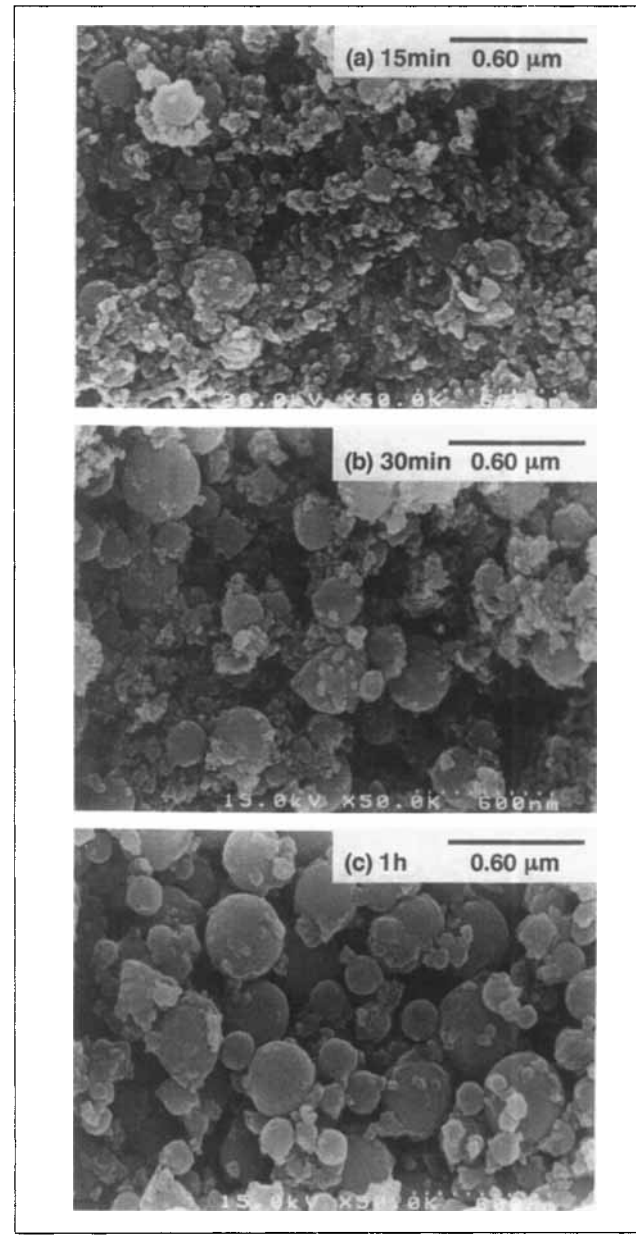

Figure 6. Scanning electron micrographs for Pr oxalate particles prepared in the ELM system at different reaction times, under the following conditions: O/A ratio = 1 and $[Pr]_0 = 500$ ppm.

t = (a) 15 min, (b) 30 min, and (c) 1 h.

$$(1-\phi')\frac{\partial A_I}{\partial t} = -k_A a_0 (A_I - A_{I,i}), \tag{6}$$

where k_A is the mass-transfer coefficient for the Ln ion through the stagnant water film, ϕ' [$= (V_{II} + V_{III})/(V_I + V_{II} + V_{III})$] is the volume fraction of the W/O emulsion drops, and a_0 is the specific surface area of the emulsion drops, which decreases with increasing stirring time.

The mass-balance equations for the extractant and extracted species in the organic membrane phase (phase II) are expressed by Eqs. 7 and 8, respectively:

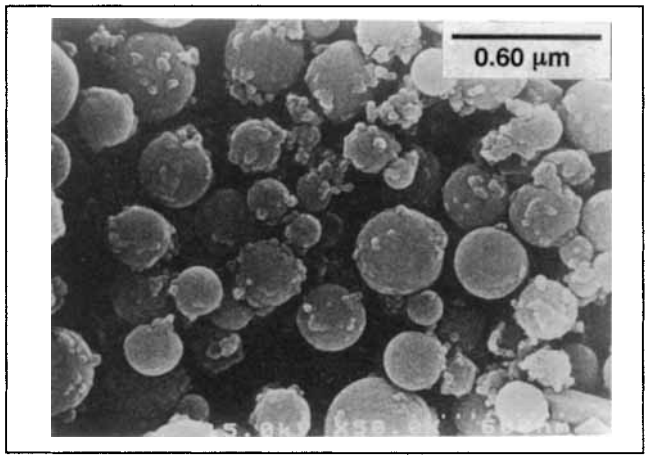

Figure 7. Scanning electron micrograph for Pr oxalate particles prepared in the ELM system with an O/A ratio = 0.5, $[Pr]_0 = 500$ ppm, and $t = 2$ h.

$$(1-\phi)\frac{\partial B}{\partial t} = D_{e,B}\left(\frac{\partial^2 B}{\partial r^2} + \frac{2}{r}\frac{\partial B}{\partial r}\right) + \frac{9\phi k_r}{R_\mu}\left(C - \frac{K_{ex}A_{III}B^3}{H_{III}^3}\right) \tag{7}$$

$$(1-\phi)\frac{\partial C}{\partial t} = D_{e,C}\left(\frac{\partial^2 C}{\partial r^2} + \frac{2}{r}\frac{\partial C}{\partial r}\right) - \frac{3\phi k_r}{R_\mu}\left(C - \frac{K_{ex}A_{III}B^3}{H_{III}^3}\right), \tag{8}$$

where $\phi[=V_{III}/(V_{II}+V_{III})]$ is the volume fraction of the total internal water droplets within the emulsion drop, $D_{e,B}$ and $D_{e,C}$ are the effective diffusivities for each of the species

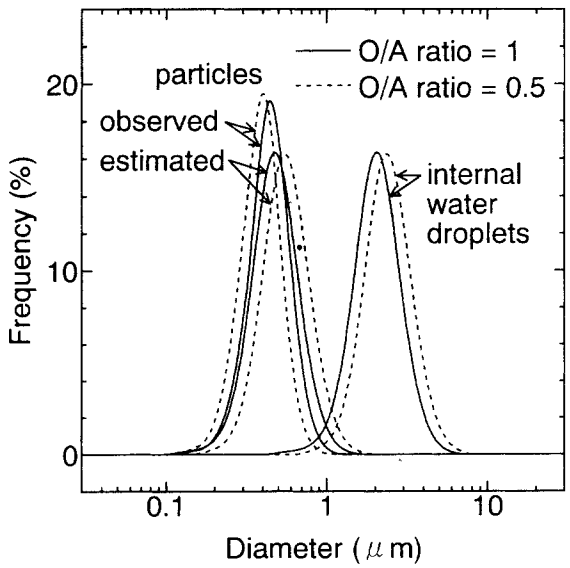

Figure 8. Size distributions for internal water droplets and Pr oxalate particles prepared in the ELM system with an O/A ratio = 1 and 0.5, $[Pr]_0 =$ 500 ppm, and $t = 2$ h.

Comparison of estimated data with observed data.

in the organic membrane phase, and R_μ is the radius of the internal water droplet.

The mass-balance equations for Ln^{3+}, H^+, oxalate ion, and oxalic acid in the internal water phase (phase III) are given by Eqs. 9–12, respectively:

$$\phi\frac{\partial A_{III}}{\partial t} = \frac{3\phi k_r}{R_\mu}\left(C - \frac{K_{ex}A_{III}B^3}{H_{III}^3}\right) - 2\phi k_p\left(A_{III}^2\left[C_2O_4^{2-}\right]^3 - K_{sp}\right)^n \tag{9}$$

$$\phi\frac{\partial H_{III}}{\partial t} = -\frac{9\phi k_r}{R_\mu}\left(C - \frac{K_{ex}A_{III}B^3}{H_{III}^3}\right) + 2\phi k_1\left([H_2C_2O_4] - \frac{\left[C_2O_4^{2-}\right]H_{III}^2}{K_1K_2}\right) \tag{10}$$

$$\phi\frac{\partial\left[C_2O_4^{2-}\right]}{\partial t} = \phi k_1\left([H_2C_2O_4] - \frac{\left[C_2O_4^{2-}\right]H_{III}^2}{K_1K_2}\right) - 3\phi k_p\left(A_{III}^2\left[C_2O_4^{2-}\right]^3 - K_{sp}\right)^n \tag{11}$$

$$\phi\frac{\partial[H_2C_2O_4]}{\partial t} = -\phi k_1\left([H_2C_2O_4] - \frac{\left[C_2O_4^{2-}\right]H_{III}^2}{K_1K_2}\right), \tag{12}$$

where k_P and K_{sp} are, respectively, the rate constant for the precipitation reaction and the solubility product for rare-earth oxalate (1.64×10^{-26} $(mol/m^3)^5$ for Pr). The term, $k_p(A_{III}^2[C_2O_4^{2-}]^3 - K_{sp})^n$ denotes the rate of precipitation, where n is the exponent of the degree of supersaturation. In many cases, $n = 2$ applies (Doremus, 1970), including the case of Cu oxalate (Hirai et al., 1996). Also, k_1 is the rate constant for dissociation of oxalic acid, and K_1K_2 is the dissociation constant ($k_1 = 5.6\times10^1$ mol/m^3 and $k_2 = 5.4\times10^{-2}$ mol/m^3). For simplicity, it is assumed here that the dissociation proceeds in one step from $H_2C_2O_4$ to $C_2O_4^{2-}$, and that only $C_2O_4^{2-}$ reacts with Ln^{3+}. In addition, the rate of dissociation is assumed to be equal to the rate of the precipitation reaction, and thus Eq. 11 becomes 0. The mass-balance equation for oxalic acid is shown by Eq. 13:

$$[H_2C_2O_4]_0 = [H_2C_2O_4] + \left[C_2O_4^{2-}\right] + 3[Ln_2(C_2O_4)_3\cdot10H_2O]. \tag{13}$$

The initial conditions are

$$A_I = A_{I,0} \quad \text{for } t = 0 \tag{14}$$

$$B = B_0,\ C = C_0,\ A_{III} = A_{III,0},\ H_{III} = H_{III,0},\ A_{III,in} = A_{III,in,0} \quad \text{for } t = 0,\ 0 \le r \le R' \tag{15}$$

$$[H_2C_2O_4] = [H_2C_2O_4]_0,\quad \left[C_2O_4^{2-}\right] = \left[C_2O_4^{2-}\right]_0. \tag{16}$$

The boundary conditions are

$$1.\ r = 0,\quad \partial B/\partial r = \partial C/\partial r = 0 \tag{17}$$

$$2.\ k_A(A_1 - A_{1,i}) = k_H(H_{1,i} - H_1)/3$$
$$= k_f(A_{1,i}B_i^3/H_{1,i}^3 - C_i/K_{ex})$$
$$= k_B(B_{r=R'} - B_i)/3 = k_C(C_i - C_{r=R'})$$
$$= -D_{e,B}(\partial B/\partial r)_{r=R'}/3 = D_{e,C}(\partial C/\partial r)_{r=R'}, \quad (18)$$

where k_B and k_C are the mass-transfer coefficients for the free extractant and extracted species, respectively, through the peripheral oil layer of the W/O emulsion drop, and R' is assumed to approximately equal R. In this model, a change of H^+ concentration in the external water phase is involved. However, mass-transfer resistance for H^+ in the external water phase film was neglected, because this step is not expected to be rate-determining. This applies particularly at the initial stage of the reaction. The preceding equations were transformed into dimensionless form and were solved, using an implicit finite difference method.

Parameter determination and comparison of the calculated results with observed results

The parameters used in the present study are shown in Table 1. Some values are as reported by Teramoto et al. (1986) for rare earths in the EHPNA-Span 80/kerosene ELM system or were obtained by Hino et al. (1997) for the EHPNA/kerosene system. Other values were determined by fitting the observed results in the time-course variations of the mole fraction of Ln^{3+} in the external water phase. The value k_A of 2.5×10^{-5} m/s gave the better simulation in the present ELM system, whereas Teramoto et al. (1986) used a value of 4×10^{-5} m/s. The values of n and k_p should be determined from the distribution profile of the particles in the W/O emulsion drop, as in the case of copper oxalate (Hirai et al., 1996). However, experimental information of the particle concentration as a function of location within the emulsion drop was not obtainable. Thus, the value of W_P (= $3A_{III,p}/H_{III,0}$, where $A_{III,p}$ is the apparent $Ln_2(C_2O_4)_3$ concentration in the internal phase), the dimensionless concentration of Ln oxalate, was estimated from the number of internal water droplets and particles, assuming that the particles were located near the emulsion drop surface and that one water droplet contained one particle. The number of droplets was calculated from the total volume of water and the droplet diameter, assuming that the size of the droplets was uniform and was identified to the mean diameter measured with the particle-size analyzer. The number of particles was calculated from the mole fraction of Ln in the internal water phase, the diameter of the particles, and the density of the solid Ln oxalate under a similar assumption. Here it was also assumed that all the Ln^{3+} ions that had moved into the internal phase were precipitated. The estimated values of W_p for the case of Pr oxalate are shown by the dotted lines (rectangle) in Figure 9. The parameter values n and k_p, which considerably affect the calculated W_p profile shown by the solid line in Figure 9, were determined by simulation of the distribution profile of Pr oxalate from the surface of the emulsion drop ($X = 1$), to fit the observed particle location. These values were assumed to be applicable for all the rare earths used in this study.

Table 1. Values of Parameters

	Ce	Pr	Nd	Sm	Gd
k_f [m/s]	9×10^{-10}	1×10^{-9}	2×10^{-9}*	8×10^{-9}*	5×10^{-8}*
K_{ex} (= k_f/k_r)	2.0×10^{-3}	6.55×10^{-3}**	9.72×10^{-3}**	0.15*	0.30*
k_A [m/s]	2.5×10^{-5}				
k_B [m/s]	4×10^{-5}*				
k_C [m/s]	$k_B\times D_C/D_B = k_B\times D_{e,C}/D_{e,B}$				
k_r [m/s]	k_f/K_{ex}				
$D_{e,B}$ [m^2/s]	1.5×10^{-10}*				
r_{CB} (= D_C/D_B or $D_{e,C}/D_{e,B}$)	0.52*				
k_P [(m^3/mol)^9/s]	1.0×10^5				
n	2				

*Teramoto et al.
**Hino et al.

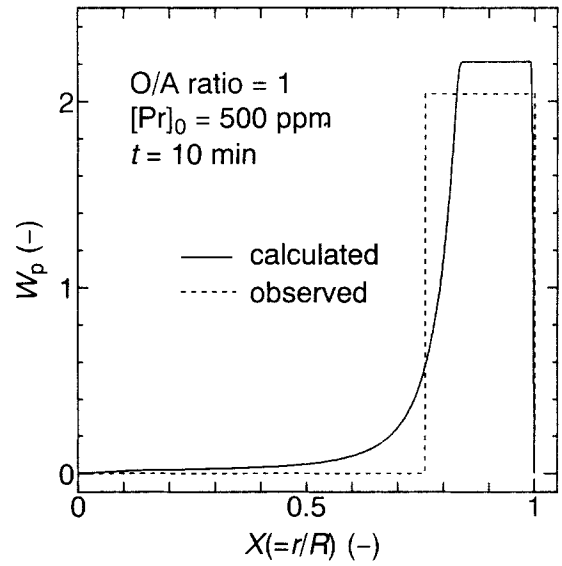

Figure 9. Location profile for Pr oxalate particles (W_p) in a W/O emulsion drop at $t = 10$ min for the case of O/A ratio = 1 and $[Pr]_0 = 500$ ppm.

Comparison of calculated data (solid line) with observed data (dotted line).

The calculated results for Pr oxalate formation are shown in Figure 10 with best-fit lines, together with the observed data (symbols). The mole fraction of Pr, in the external water phase, was successfully expressed, using the parameters obtained, except for the case $[Pr]_0 = 1{,}000$ ppm (7.1 mmol/L). For this condition, the quantity of oxalic acid in the internal phase is insufficient to strip Pr^{3+} and to make oxalate effectively, and thus the transport rate is likely to be decreased. A similar calculation for the mole fraction of Ln^{3+} in the external phase with corresponding values of k_f and K_{ex} was carried out for the other rare earths, Ce, Nd, Sm, and Gd ($[Ln]_0$ = 500 ppm = 3.1–3.7 mmol/L), and showed good agreement with the observed results.

Control of particle size

Figure 9 shows that the calculated value of W_p saturates at a maximum value of 2.21, as shown by the solid line. The value of $W_p = 2.21$ corresponds to the condition at which all

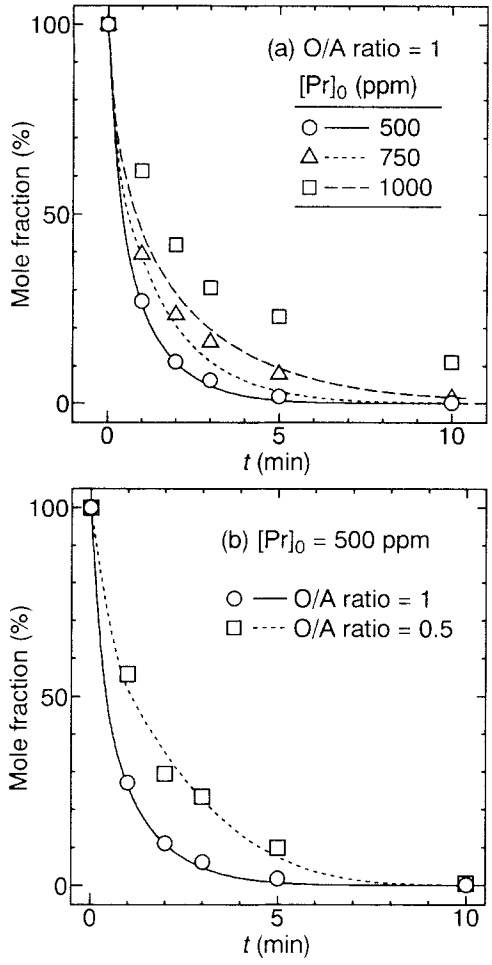

Figure 10. Time-course variations for mole fraction of Pr ion in the external water phase.

Comparison of calculated data (lines) with observed data (symbols). Effect of (a) $[Pr]_0$ and (b) O/A ratio.

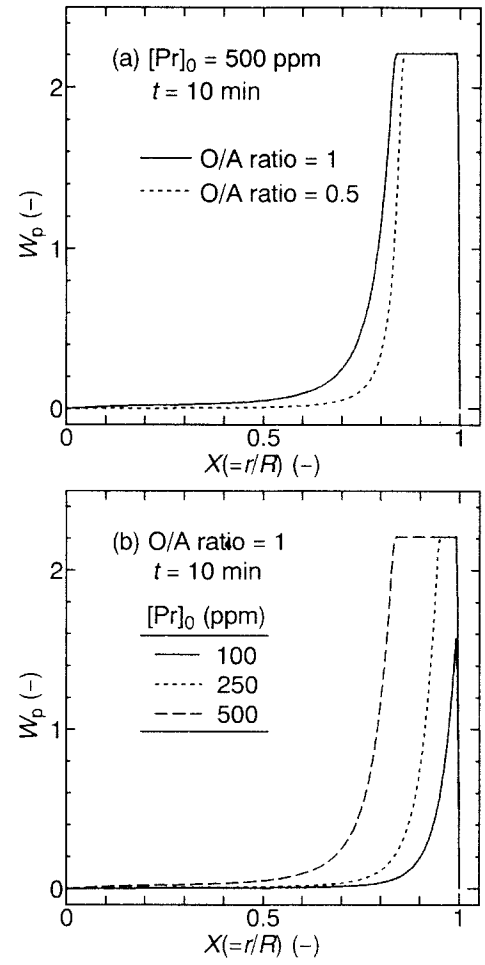

Figure 11. Estimated location profiles for Pr oxalate particles (W_p) in a W/O emulsion drop at t = 10 min.

Effect of (a) O/A ratio and (b) $[Pr]_0$.

the oxalic acid in one water droplet is consumed stoichiometrically for oxalate particle formation, since $H_{III,0}$ is assumed to be 4.52×10^{-2} mol/L from the pH measurement. In such a saturated region, the quantity of rare-earth oxalate in one droplet is governed by the feed quantity of oxalic acid, even when an excess quantity of metal ions may be supplied in the droplet. Thus, the particle-size distribution can be estimated from the size distribution of the water droplets and the quantity of oxalic acid in each droplet in this "saturated" case. That is, the histogram of droplet-size distribution gives the quantity of oxalic acid and thus the quantity of Pr oxalate in a droplet for each diameter range, which enables calculation of the particle size by using the density of the solid Pr oxalate. As shown in Figure 8, the estimated particle-size distribution shows good agreement with the observed particle size.

At an O/A ratio of 0.5, some difference in the particle location is predicted by the simulation, as shown in Figure 11a. In the larger region of X, however, the value of W_p is saturated at 2.21, and thus the particle size is assumed to be dominated by the quantity of oxalic acid in one water droplet, as in the case of the O/A ratio = 1. The particle size thus estimated, as shown in Figure 8, is slightly greater than the observed data. The size distribution measured with the particle-size analyzer is probably affected by the smaller particles that still remain even at t = 2 h, as shown in Figure 7.

These findings clearly show that the size control of oxalate particles, by controlling the distribution of Ln^{3+} ions into the internal droplets, is actually feasible. Two approaches were carried out. One is the reduction of the feed Pr concentration, so that not all of the feed oxalic acid in the droplets is consumed. The effect of $[Pr]_0$ on W_p is shown in Figure 11b. The saturated region is also seen at $[Pr]_0$ = 250 ppm (1.75 mmol/L), but not at 100 ppm (0.7 mmol/L). The particle-size distribution at 100 ppm is thus shifted toward the smaller diameter region, as shown in Figure 12a. The maximum particle size, at this condition, can be estimated as 0.41 μm from the maximum value of W_p at X = 1 in Figure 11b, which seems to be consistent with the observed size distribution. A second approach is to change the size of the internal water droplets in order to change the quantity of oxalic acid in each water droplet. The droplet size was enlarged by decreasing the Span 83 concentration and the agitation speed of the homogenizer (about 2,000 rpm), as shown in Figure 12b. At the condition of $[Pr]_0$ = 500 ppm, a saturated region for W_p was observed

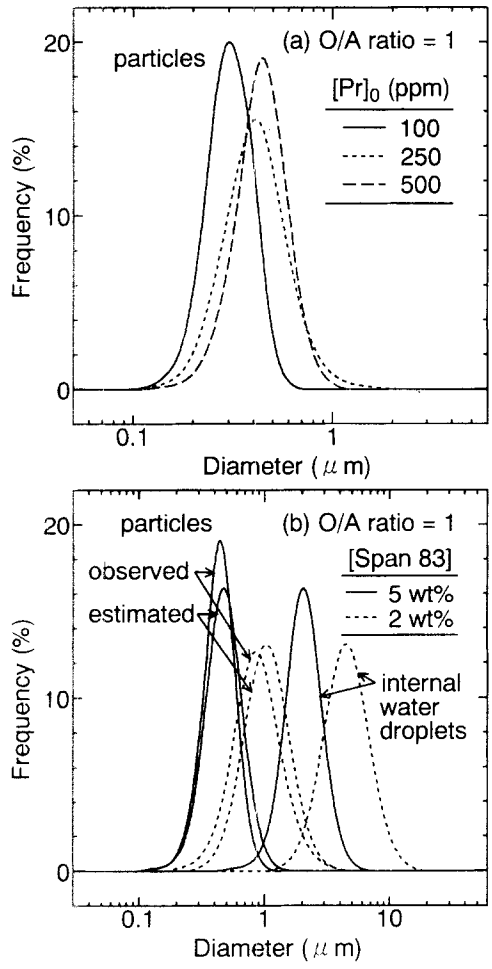

Figure 12. Size distributions for internal water droplets and Pr oxalate particles, prepared in the ELM system with an O/A ratio = 1 and $t = 2$ h.

Effect of (a) $[Pr]_0$ and (b) [Span 83].

in the calculated particle location profile in this ELM system, as with the ELM system with the smaller water droplets. The particles of larger size, shown in Figure 13, were formed as expected, and the size distribution agreed well with the estimated particle-size distribution as shown in Figure 12b.

Conclusions

Rare-earth oxalate particles were prepared by using an emulsion liquid membrane (ELM, W/O/W emulsion) system, consisting of Span 83 (sorbitan sesquioleate) as surfactant and EHPNA (2-ethylhexylphosphonic acid mono-2-ethylhexyl ester) as a cation carrier. The mechanism of formation for the particles and the factors determining the particle size were investigated with the following results:

1. Submicron-sized well-defined spherical oxalate particles of Ce, Pr, Nd, Sm, and Gd were obtained via the formation of primary particles of about 20 nm in size, followed by aggregation. These oxalate particles gave corresponding fine oxide particles by calcination. For the case of La, Dy, and Y, less spherical or rather tabular particles were formed, while oxalate particles of Yb were not obtained.

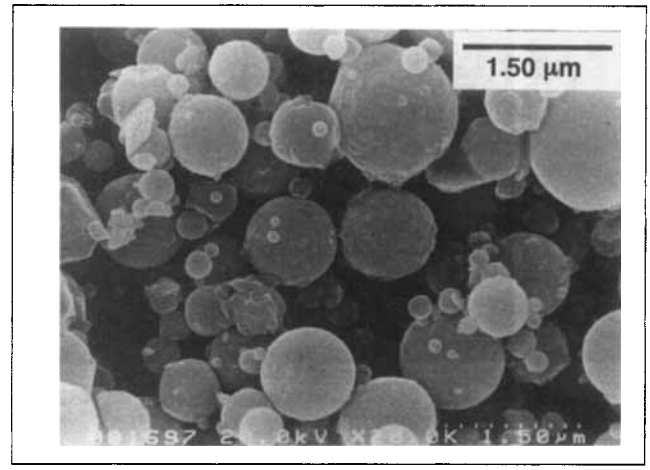

Figure 13. Scanning electron micrograph for Pr oxalate particles prepared in the ELM system having large internal water droplets (mean diameter: 4.18 μm) with an O/A ratio = 1, $[Pr]_0$ = 500 ppm, and $t = 2$ h.

2. A simulation study, based on a model of the transport mechanism of rare-earth ions through the organic membrane, was successfully carried out. This study suggested that the particle size was controlled by the distribution of rare-earth ions into the internal water droplets, and this was also confirmed by the experimental results. Control of the particle size is shown to be feasible by control of the feed rare-earth concentration and the size of the internal water droplets.

Acknowledgments

The authors are grateful to the Department of Chemical Science and Engineering, Osaka University, for scientific support in respect of the "Gas-Hydrate Analyzing System (GHAS)" constructed by a supplementary budget of 1995, and to the financial support by Grant-in-Aid for Scientific Research (Nos. 08455357 and 09650829) from the Ministry of Education, Science, Sports and Culture, Japan. One of the authors (T. H.) Acknowledges the financial support by The Foundation "Hattori-Hokokai" and by The Sumitomo Foundation.

Notation

D_B = diffusivity of extractant in organic membrane phase, m^2/s
D_C = diffusivity of Ln-extractant complex in organic membrane phase, m^2/s
K_{ex} = extraction equilibrium constant
k_f = rate constant for forward reaction, m/s
k_H = mass-transfer coefficient for H^+ through external water stagnant film, m/s
k_r = rate constant for reverse reaction, m/s
R = radius of W/O emulsion drop, m
R' = radial distance from the center of the W/O emulsion drop to the peripheral oil layer, m
r = radial distance, m
t = reaction time, min
V = volume, m^3
W_p = dimensionless concentration of rare-earth oxalate in internal water phase, $3A_{III,p}/H_{III,0}(A_{III,p} = [Ln_2(C_2O_4)_3])$
X = dimensionless length scale of emulsion drop, r/R

Subscripts

0 = initial value
i = interface between external water phase and W/O emulsion drop

Literature Cited

Davey, R. J., and T. Hirai, "The Preparation of Calcium Carbonate in an Emulsified Liquid Membrane," *J. Cryst. Growth*, **171**, 318 (1997).

Doremus, R. H., "Precipitation and Crystal Growth from Solution," *Croat. Chem. Acta*, **42**, 293 (1970).

Doyle, F. M., "Integrating Solvent Extraction with the Processing of Advanced Ceramic Materials," *Hydrometallurgy*, **29**, 527 (1992).

Doyle, F. M., H. Choi, E. Antico, M. Valiente, and J.-C. Lee, "Influence of Organic Phase Speciation on the Characteristics of Yttria Precursor Powders Precipitated from Yttrium-Loaded D2EHPA Solutions," *Processing Materials for Properties*, H. Henein and T. Oki, eds., TMS, Warrendale, PA, p. 545 (1993).

Hino, A., S. Nishihama, T. Hirai, and I. Komasawa, "Practical Study of Liquid-Liquid Extraction Process for Separation of Rare Earth Elements with Bis(2-ethylhexyl)phosphinic Acid," *J. Chem. Eng. Jpn.*, **30**, in press (1997).

Hirai, T., K. Nagaoka, N. Okamoto, and I. Komasawa, "Preparation of Copper Oxalate Fine Particles Using Emulsion Liquid Membrane System," *J. Chem. Eng. Jpn.*, **29**, 842 (1996).

Hirai, T., S. Hariguchi, I. Komasawa, and R. J. Davey, "Biomimetic Synthesis of Calcium Carbonate Particles in a Pseudovesicular Double Emulsion," *Langmuir*, **13**, in press (1997).

Konishi, Y., S. Asai, and T. Murai, "Precipitation Stripping of Neodymium from Carboxylate Extractant with Aqueous Oxalic Acid Solutions," *Ind. Eng. Chem. Res.*, **32**, 937 (1993a).

Konishi, Y., S. Asai, and T. Murai, "Characterization of Noedymium Oxalate Precipitated from 2-Ethylhexyl Phosphoric Acid Mono-2-Ethylhexyl Ester Solution," *Metall. Trans. B*, **24B**, 537 (1993b).

Lee, J.-C., and F. M. Doyle, "Precipitation of Yttrium Oxalate from Di-2-ethylhexyl Phosphoric Acid Solution," *Rare Earths: Resources, Science, Technology and Applications*, R. G. Bautista and N. Jackson, eds., TMS, Warrendale, PA, p. 139 (1991).

Majima, H., T. Hirato, Y. Awakura, and T. Hibi, "Preparation of Monosized Ultrafine Particles of Precious Metals Utilizing an Emulsion-Type Liquid Membrane Technique," *Metall. Trans. B*, **22B**, 397 (1991).

Sanuki, S., A. Sugiyama, M. Tunekawa, K. Kadomachi, and K. Arai, "Precipitation Stripping of Samarium Oxalate from Organic Solution Containing Acid Type Extractant by Oxalic Acid," *J. Jpn. Inst. Metals*, **58**, 1271 (1994).

Stewart, A. C., and G. A. Davies, "Liquid Surfactant Membrane Systems for Extraction from Dilute Solutions," *S. Africa J. Chem. Eng.*, **4**, 41 (1992).

Teramoto, M., T. Sakai, K. Yanagawa, M. Ohsuga, and Y. Miyake, "Modeling of the Permeation of Copper through Liquid Surfactant Membranes," *Sep. Sci. Technol.*, **18**, 735 (1983).

Teramoto, M., T. Sakuramoto, T. Koyama, H. Matsuyama, and Y. Miyake, "Extraction of Lanthanoids by Liquid Surfactant Membranes," *Sep. Sci. Technol.*, **21**, 229 (1986).

Yang, M., G. A. Davies, and J. Garside, "The Preparation of Solids in a Liquid Membrane Emulsion: The Control of Particle Size," *Powder Technol.*, **65**, 235 (1991).

Yoon, J. H., and F. M. Doyle, "Precipitation of Rare-Earth Powders from Aqueous Solutions and Emulsions," *Innovations in Materials Processing Using Aqueous, Colloid, and Surface Chemistry*, F. M. Doyle, S. Raghavan, P. Somasundaran, and G. W. Warren, eds., TMS, Warrendale, PA, p. 195 (1988).

Yoon, J. H., and F. M. Doyle, "Preparation of Lanthanide Oxalate Powders Using Carboxylate-Based Emulsions," *Light Metals 1990*, C. M. Bickert, ed., TMS, Warrendale, PA, p. 991 (1990).

Manuscript received May 29, 1997, and revision received Aug. 22, 1997.